



Published in final edited form as:

Nat Genet. ; 44(3): 343–347. doi:10.1038/ng.1068.

Epigenetic repression of cardiac progenitor gene expression by Ezh2 is required for postnatal cardiac homeostasis

Paul Delgado-Olguín¹, Yu Huang¹, Xue Li^{2,3,4}, Danos Christodoulou⁵, Christine E. Seidman^{5,6}, J.G. Seidman⁵, Alexander Tarakhovsky⁷, and Benoit G. Bruneau^{1,8,9}

¹Gladstone Institute of Cardiovascular Disease, San Francisco, CA, USA

²Urological Diseases Research Center, Children's Hospital Boston, 300 Longwood Avenue, Boston, Massachusetts, USA

³Department of Pathology, Harvard Medical School, Boston, MA, USA

⁴Harvard Stem Cell Institute, Cambridge, MA, USA

⁵Department of Genetics, Harvard Medical School, Boston MA 02115 USA

⁶Howard Hughes Medical Institute, Division of Cardiovascular Medicine, Brigham and Women's Hospital, Boston, MA, USA

⁷Laboratory of Lymphocyte Signaling, The Rockefeller University, New York, NY, USA

⁸Department of Pediatrics, Cardiovascular Research Institute. University of California, San Francisco, CA, USA

⁹Institute for Regeneration Medicine, University of California, San Francisco, CA, USA

Abstract

Adult-onset diseases can be associated with *in utero* events, but mechanisms for this remain unknown^{1,2}. The polycomb histone methyltransferase, Ezh2, stabilizes transcription by depositing repressive marks during development that persist into adulthood^{3–9}, but its function in postnatal organ homeostasis is unknown. We show that Ezh2 stabilizes cardiac gene expression and prevents cardiac pathology by repressing the homeodomain transcription factor *Six1*, which functions in cardiac progenitors but is stably silenced upon cardiac differentiation¹⁰. Ezh2 deletion in cardiac progenitors caused postnatal myocardial pathology and destabilized cardiac gene expression with activation of *Six1*-dependent skeletal muscle genes. *Six1* induced cardiomyocyte

Users may view, print, copy, download and text and data- mine the content in such documents, for the purposes of academic research, subject always to the full Conditions of use: http://www.nature.com/authors/editorial_policies/license.html#terms

Correspondence should be addressed to B.G.B. (bbruneau@gladstone.ucsf.edu).

Accession codes.

Microarray data can be accessed at GEO. Accession ID: GSE30076

RNA-Seq data can be accessed at GEO. Accession ID: GSE34274

AUTHOR CONTRIBUTIONS

P.D.-O. designed the study with B.G.B. and performed most of the experiments; Y.H. performed echocardiography; X.L. provided essential information prior to publication; X.L. and A.T. provided mouse lines; D.C. generated and analyzed RNAseq data with C.E.S. and J.G.S.; P.D.-O. and B.G.B. wrote the paper with input from all the authors.

COMPETING FINANCIAL INTERESTS

The authors declare no competing interests.

hypertrophy and skeletal muscle gene expression. Furthermore, genetically reducing *Six1* levels rescued the pathology of *Ezh2*-deficient hearts. Thus, *Ezh2*-mediated repression of *Six1* in differentiating cardiac progenitors is essential for stable postnatal heart gene expression and homeostasis. Our results suggest that epigenetic dysregulation in embryonic progenitor cells predisposes to adult disease and dysregulated stress responses.

Cardiac hypertrophy results from integrating numerous signalling pathways that culminate in well-described transcriptional networks¹¹. In humans, variation in hypertrophy is induced by similar stimuli across populations. While genetic variation contributes¹², epigenetic regulatory mechanisms, particularly during embryonic development are largely unexplored,^{1,2}. The heart may be particularly sensitive to early events, as turnover of human cardiomyocytes is limited over a lifetime¹³. Epigenetic regulation via histone methylation stabilizes transcriptional programs in embryonic progenitors and their differentiated descendants^{3,4}, and is likely critical for establishing and maintaining gene expression and stress responses throughout life. Polycomb complexes are candidates for stabilizing cardiac gene expression. They control cell identity and epigenetic memory in other contexts⁵. *Ezh2*, the major histone methyltransferase of the polycomb repressor complex 2 (PRC2), trimethylates histone H3 at lysine 27 (H3K27me3). *Ezh2* is essential for embryonic development⁵⁻⁹, but its function in organogenesis or postnatal organ maintenance is unknown.

Ezh2, and the related H3K27 methyltransferase *Ezh1*^{14,15} are expressed in cardiomyocytes (Supplementary Fig. 1), and H3K27me3 levels increase in cardiac progenitor cells as they differentiate into cardiomyocytes (Supplementary Fig. 2). This suggests that PRC2 functions in the transition from cardiac progenitor to differentiated cardiomyocyte.

To determine the function of PRC2 in mouse heart, we inactivated *Ezh2* by Cre-mediated recombination in a subpopulation of cardiac progenitors known as the anterior heart field (AHF), which contribute to the right ventricle, interventricular septum, and outflow tract¹⁶. Mice with loxP sites flanking the catalytic domain-encoding region of *Ezh2* (*Ezh2^{fl/fl}*)⁶ were crossed with mice expressing Cre recombinase under the *Mef2cAHF* enhancer (*Mef2cAHF::Cre*), which is active from embryonic day 7.5 (E7.5)¹⁶. AHF progenitors with inactivated *Ezh2* failed to increase H3K27me3 levels as they differentiated into cardiomyocytes (Supplementary Fig. 2c-h), resulting in decreased *Ezh2* and over 80% of right, but not left, ventricular cardiomyocytes with decreased H3K27me3 (Supplementary Fig. 3a,b), suggesting that *Ezh2* is the major H3K27 histone methyltransferase in the AHF. H3K27me3 levels were not reduced in endothelial cells (Supplementary Fig. 2d). Mice with *Ezh2*-deficient AHF cells developed normally structured hearts (Supplementary Fig. 4). However, *Ezh2*-deficient hearts became enlarged after birth, with increased heart weight to tibia length ratios (Fig. 1a,b). Cardiac enlargement was restricted to the right ventricular wall, in which cardiac myocytes were massively hypertrophied, with an almost fourfold increase in cross-sectional area (Fig. 1c,d). Echocardiography confirmed right ventricular enlargement and showed mild pulmonary stenosis (Supplementary Table 1). Cardiomyocytes were already enlarged in E20 fetuses (Supplementary Fig. 5a), ruling out altered hemodynamics as a primary cause of hypertrophy. *Ezh2*-deficient right ventricles

were fibrotic (Fig. 1e,f), and the endocardium was invaginated into the ventricular myocardium (Fig. 1g), resembling ventricular non-compaction^{12,17}. Thus loss of *Ezh2* in cardiac precursors leads to cardiac hypertrophy and fibrosis.

We examined altered gene expression in *Ezh2*-deficient adult hearts. The hypertrophy-associated genes^{18,19} *Nppa*, *Nppb*, and *Myh7*, as well as the profibrotic genes *Tgfβ3*, *Postn* and *Spp1* were highly upregulated (Fig. 2a,b). Immunofluorescence detected low levels of Tgfβ3 in the perinuclear region of wild-type cardiac myocytes, while it was enriched in the extracellular region in *Ezh2*-deficient hearts (Fig. 2c). Thus, *Ezh2* might suppress gene expression that promotes cardiac hypertrophy and fibrosis.

If *Ezh2* function were epigenetic, a sustained requirement for its activity would be anticipated. To address this, *Ezh2* was deleted in differentiating ventricular myocytes using ventricular myocyte-specific *Nkx2.5::Cre* transgenic mice^{20,21}, which express Cre only after cardiomyocytes begin to differentiate. *Ezh2^{fl/fl};Nkx2.5::Cre* mice had mild cardiomyocyte hypertrophy and increased *Myh7* mRNA levels (Supplementary Fig. 6b,e), perhaps due to reduced *Nkx2.5::Cre*-mediated recombination efficiency^{20,21} (Supplementary Fig. 3c,d), or to a critical window of activity of *Ezh2* during early cardiac progenitor differentiation. Thus, *Ezh2* functions in cardiomyocyte progenitors, with long-term consequences.

We hypothesized *Ezh2*-mediated H3K27me3 directly represses fetal genes, and reactivation in *Ezh2*-deficient hearts results from loss of epigenetic repression. At the *Nppa* promoter¹⁹, occupancy of the PRC2 core subunit suppressor of zeste 12 homolog (*Suz12*) and H3K27me3 was decreased in *Ezh2* mutant hearts, and acetylated histone H3 (AcH3, activating mark) and RNA polymerase II (PolIII) were increased (Fig. 2d, Supplementary Fig. 7). These results suggest *Ezh2* directly represses fetal gene expression to maintain cardiac homeostasis.

The global gene expression profile of adult *Ezh2*-deficient right ventricles was determined by RNA sequencing (RNA-seq) and DNA microarrays. With a stringent $P < 0.001$ and fold-change cutoff of > 1.4 , 1,132 genes were upregulated, and 1,800 downregulated (Supplementary Table 2). Consistent with hypertrophy and fibrosis, myocardial remodelling-associated genes (e.g., *Nppa*, *Nppb*) and atrial-specific genes (*Sln*, *Myl7*), were upregulated in *Ezh2*-deficient hearts (Fig. 2e). Genes involved in signalling pathways mediating myocardial remodelling were also misregulated (Supplementary Table 3). Gene Ontology classification showed surprisingly that many misregulated genes encode skeletal muscle-specific contractile proteins and developmental regulators (Fig. 2f), including some that are normally induced in cardiac hypertrophy (e.g., *Acta1*). Thus, *Ezh2* is required to stabilize postnatal cardiac gene expression.

In pluripotent cells, Polycomb complexes repress transcription factors regulating cell differentiation and development⁵. We hypothesized *Ezh2*-mediated repression of key transcription factors is essential to stabilize cardiac gene expression. Our analyses showed increased expression of the homeodomain transcription factor *Six1*²² and its coactivators, *Eya1*, *Eya2*, and *Eya4*^{23,24} (Fig. 2e; Supplementary Table 2). *Six1* functions in non-cardiac cell types, including skeletal muscle. Indeed, many ($P < 2 \times 10^{-8}$) genes misregulated in *Ezh2*-

deficient hearts are direct *Six1* targets in differentiating skeletal myoblasts (Fig. 2e)²⁵. *Six1* targets were preferentially misregulated over non-*Six1* targets (Fig. 2g). Levels of *Six1*, *Eya1*, and some skeletal muscle genes were also increased in *Ezh2^{fl/fl};Nkx2.5::Cre* hearts (Supplementary Fig. 6e). *Six1* functions in early cardiac progenitors, but not in differentiating cardiomyocytes¹⁰ and remains silent in developing and postnatal heart (Fig. 3b,c; 6d; Supplementary Fig. 8). Upon loss of *Ezh2*, *Six1* might activate transcription of a skeletal muscle genes subset in cardiomyocytes, contributing to instability of cardiac gene expression.

We addressed the relevance of increased *Six1* expression in deregulating gene expression in *Ezh2*-deficient hearts. Quantitative real time PCR (QRT-PCR) confirmed *Six1* de-repression in early developing ventricular myocardium (E10) and exclusively in the adult *Ezh2*-deficient right ventricle (Fig. 3a), consistent with specific repression by *Ezh2*. At E13.5, in newborn, and adult hearts, *Six1* expression was increased in *Ezh2*-deficient right ventricular myocardium (Fig. 3b,c; Supplementary Fig. 8), and *Eya1* was derepressed exclusively in adult cardiomyocytes (Fig. 3b). Furthermore, upon loss of *Ezh2*, *Six1* was expressed in nuclei of adult cardiomyocytes that concomitantly expressed the skeletal muscle-specific *Six1* target *Actn3* (Fig. 3c).

To determine if *Six1* and *Eya1* are targets for PRC2-mediated repression, we performed chromatin immunoprecipitation. In *Ezh2*-deficient adult hearts, H3K27me3 and Suz12 were depleted at the *Six1*, but not *Eya1*, promoter (Fig. 3d, not shown). PolII and acetylated histone H3 (AcH3) were enriched, consistent with *Six1* derepression. Thus, PRC2 epigenetically represses *Six1* expression.

Six1 expression is rapidly extinguished upon differentiation of cardiac progenitors¹⁰, but its derepression in *Ezh2^{fl/fl};Mef2cAHF::Cre* hearts suggests an expression potential in differentiated myocardium. Computational analysis of the *Six1* locus identified a highly conserved sequence in the *Six1* 5' non-coding region with putative binding motifs for cardiac development regulators *Nkx2-5*, *GATA4* and *Mef2c* (Fig. 4a). To test its potential to drive cardiac expression, this conserved element was fused to a *LacZ*-reporter driven by the *Hsp68* promoter, and the resulting reporter construct (Fig. 4b) was injected in mouse zygote pronuclei. About 50% of transient transgenic embryos (6/12) showed β -galactosidase activity in the myocardium (Fig. 4c–e), suggesting that this enhancer is active in the heart when not in its endogenous repressed genomic location. This agrees with suppression of a cardiac expression-potential of the *Six1* locus in differentiating cardiac progenitors.

We investigated the effect of persistent *Six1* and *Eya1* expression in cardiomyocytes on hypertrophy. Overexpression of *Six1*, with or without *Eya1*, in cultured neonatal mouse cardiomyocytes resulted in hypertrophy comparable to that induced by the potent hypertrophic agonist, Endothelin-1 (Fig. 5a). In addition, *Six1* and *Eya1* synergistically activated fetal cardiac and skeletal muscle gene expression (Fig. 5b; Supplementary Fig. 9).

To determine if *Six1* derepression causes the phenotype of mice with *Ezh2*-deficient hearts, we reduced *Six1* levels. *Ezh2^{fl/fl};Mef2cAHF::Cre* mice were bred onto a heterozygous *Six1-LacZ* knock-in background²³, and cardiomyocyte hypertrophy and fibrosis were analyzed in

adult mice. Reducing levels of *Six1* by 50% in *Ezh2*-deficient hearts significantly normalized heart size, as measured by heart weight to tibia length ratios (Fig. 6a). Furthermore, cardiomyocyte size and the levels of *Tgfb3* and fibrosis were almost completely rescued (Fig. 6b,c; Supplementary Fig. 10). Skeletal muscle genes, the hypertrophy marker *Myh7*, and the profibrosis factors *Tgfb3* and *Postn*, also returned to normal expression levels (Fig. 6d; Supplementary Fig. 10). Residual *Six1* (Fig. 6d) might account for the persistent phenotype. Evidence points to a direct effect of *Six1* misregulation in myocardium and rule out secondary effects due to outflow tract pressure overload. *Six1* and its target *Actn3* are coexpressed in *Ezh2*-deficient cardiomyocytes (Fig. 3c), and *Six1* occupied the *Nppa*, *Myl1* and *Tgfb3* locus in *Ezh2*-deficient hearts (Supplementary Fig. 11). In addition, mild thickening of the pulmonary valve leaflets in *Ezh2^{fl/fl};Mef2cAHF::Cre* adult hearts (Supplementary Fig. 12) was not present in already hypertrophied fetal hearts (Supplementary Fig. 5b), and was not rescued upon decreasing *Six1* levels (Supplementary Fig. 12), despite a normalization of hypertrophy and fibrosis (Fig. 6b–c). Thus, myocardial deregulation of *Six1* alone is the major cause of myocardial hypertrophy and fibrosis in the *Ezh2*-deficient heart.

We uncovered a finely regulated epigenetic regulatory mechanism in which *Ezh2*-mediated stable repression of *Six1* in differentiating embryonic cardiac progenitors is essential for normal cardiac growth and stress-responsiveness in the adult. *Ezh2* modulates a feed-forward pathway repressing fetal gene expression, which is reinforced by repression of *Six1*. (Supplementary Fig. 13). This represents a novel pathway for regulating cardiac growth: neither *Ezh2* nor *Six1* is upregulated in hearts subjected to hypertrophic stimuli (Supplementary Fig. 14). Repressing *Six1* is required to stabilize cardiac gene expression by preventing activation of skeletal muscle genes in cardiac muscle. *Ezh2* loss is likely insufficient to activate this program merely acting as a “brake”, but reactivation of *Six1* (the “gas pedal”) and expression of its targets results in pathologic cardiac remodelling with hypertrophy and fibrosis. Mutations in *EYA4* cause cardiomyopathy in humans²⁴, strengthening the idea that control of Six-Eya function is critical for normal cardiac homeostasis. Our results suggest *Ezh2*-mediated *Six1* repression in cardiac progenitors stabilizes postnatal cardiac gene expression, illustrating the importance of epigenetic regulation early in development and its implications in postnatal organ homeostasis.

METHODS

Mice

The following mice strains were used: *Ezh2^{fl/fl}*, *Mef2cAHF::Cre*, *Nkx2-5::Cre*, and *Six1^{LacZ/+}*. All animal experiments were conducted following guidelines established and approved by the UCSF Institutional Animal Care and Use Committee.

Plasmids

Six1 and *Eyal* expression vectors were constructed by cloning PCR-amplified full-length cDNAs into pCDNA3.1/V5-His TOPO (Invitrogen).

Cardiac hypertrophy induction

Isoproterenol (60 mg/kg body weight) was administered for 14 days in 9 weeks old mice using ALZET osmotic minipumps, which were surgically implanted subdermally. As control mice were implanted with PBS-filled minipumps. 5 mice per genotype were treated.

Protein analysis

Immunostaining and *in situ* hybridization procedures were carried out by standard protocols. For immunostaining, cryosections were incubated with the next primary antibodies: anti-trimethyl-Histone H3 (Lys 27) (Millipore 07-449, 1:3000), histone H3 trimethyl Lys9 (39161 Active Motif, 1:1000), alpha tropomyosin (CH1 monoclonal, Hybridoma bank, 1:100), cardiac troponin t (Thermo Scientific, 1:1000) Pab to Vimentin (GP53 Progen, 1:500), Tgf β 3 (sc-83 Santa Cruz Biotechnology, 1:100), Alpha-actinin 3 (Epitomics, 1:100), Six1²⁵ (1:100), Isl1 (Developmental Studies Hybridoma Bank, 1:250), Ezh2 (Active Motif, 1:200), and Ezh1 (Abcam, 1:200). Cultured myocytes were incubated with the next primary antibodies: β -galactosidase (Abcam, 1:100) and anti-V5 (R960-25 Invitrogen, 1:100). After incubation with primary antibodies, the sections were washed 3 \times with PBS, incubated with Alexa Fluor-conjugated secondary antibodies (Invitrogen, 1:500), washed and mounted with Prolong gold with 4,6-diamidino-2-phenylindole (Invitrogen) to counterstain nuclei. Fluorescent signal for vimentin and Tgf β 3 was quantified as Mean Gray Value with ImageJ. Multiple sections from at least three hearts per genotype were analyzed. The next antibodies were used for Western blot: anti-Ezh2 (Cell Signalling, 1:1000) and anti-GAPDH (Santa Cruz Biotechnology, 1:1000).

Gene expression analysis

RNA was isolated from the right ventricle and interventricular septum and treated with DNaseI. cDNA was prepared with the SuperScript III First Strand Synthesis Kit (Invitrogen). 10 pg of cDNA were used for quantitative real-time amplification with the next TaqMan probes. *Nppa* Mm01255747_g1, *Nppb* Mm00435304_g1, *Myh7* Mm00600555_m1, *Tgf β 3* Mm01307950_m1, *Postn* NM_015784.2, *Spp1* Mm00436767_m1, *Six1* Mm00808212_m1, *Eya1* Mm00438796_m1, *Myh8* Mm01329494_m1, *Myl1* Mm00659043_m1, *Myl2* Mm00440384_m1, *Myl4* Mm00440377_m1, *Mylpf* Mm00443940_m1, *Tnni1* Mm00502426_m1, *Actn3* Mm00496495_m1 and *Tnni2* Mm00437157_g1. *In situ* hybridization on whole mount embryos and on 10 μ m paraffin sections was performed as previously reported. RNA antisense probes were labeled with digoxigenin-coupled UTP. After hybridization, samples were washed and incubated with alkaline phosphatase-coupled anti-digoxigenin antisera (Roche). Signal was developed with BM purple (Roche).

Cell measurements

Cryosections were fixed in 4% PFA for 5 min, incubated with 5 μ g/ μ l wheat germ agglutinin, Alexa Fluor[®] 594 conjugate (W11262 Invitrogen) for 10 min and washed 3 \times ten min each with PBS. Sections were then mounted with Prolong gold with 4,6-diamidino-2-phenylindole (Invitrogen). Micrographs were taken from right and left ventricles. The cross sectional area of myocytes was measured using ImageJ. At least 100 cardiomyocytes were

measured per image. Multiple sections obtained from at least three hearts per genotype were analyzed. The same method was used to measure alpha tropomyosin-stained cardiomyocytes in culture. At least 50 cells were measured from three biological replicates.

Microarray analysis and RNA-seq

RNA was isolated from the right ventricle and interventricular septum of five *Ezh2^{fl/fl}* and five *Ezh2^{fl/fl};Mef2cAHF::Cre* mice. Affymetrix mouse Gene ST 1.0 arrays were hybridized and scanned according to the manufacturer's recommendations. Linear models were fitted for each gene on *Ezh2^{fl/fl};Mef2cAHF::Cre* vs *Ezh2^{fl/fl}* samples to derive the mutant effect using the limma package in R/Bioconductor. Moderated t-statistics and the associated P-values were calculated, adjusting for multiple testing by controlling for false discovery rate with the Benjamini-Hochberg method and for family-wise error rate using the Bonferroni correction (adjP). Genes with adjP<0.05 were considered differentially expressed. RNAseq was performed as previously described in RNA from the right ventricle of five hearts per genotype²⁶. Gene ontology analysis was performed using GO Elite.

Chromatin immunoprecipitation

Chromatin was isolated from the right ventricle and the interventricular septum with the Imprint Chromatin Immunoprecipitation Kit (Sigma), following manufacturer instructions. The immunoprecipitated chromatin, input and IgG-bound chromatin were analyzed by qPCR using TaqMan probes for the *Nppa* core promoter, *Nppa* distal promoter, *Six1* core promoter, *Eyal* core promoter, and the *Srf* core promoter (Supplementary Table. 4)

Cardiomyocyte culture and infection

Newborn mouse cardiomyocytes were isolated and maintained using the Neonatal Cardiomyocyte Isolation System (Cellutron) as recommended by the manufacturer.

Cardiomyocytes were seeded in 8 well chamberslides 48 h before infection. Cells were infected with 5.5×10^8 IFU of *Six1*-encoding adenovirus and 1.2×10^8 IFU of *Eyal*-encoding adenovirus per well. Cells were fixed and stained 48 h post infection.

For induction of cardiomyocyte hypertrophy, 0.2 mM of Endothelin 1 (Sigma) was added to the culture media. Cells were exposed for 48 h.

Adenoviruses

For generation of adenoviral vectors, *Six1* and *Eyal* cDNAs were cloned into pAd/CMV/V5-DEST (Invitrogen).

Viral particles were generated using the ViraPower Adenoviral Expression System. Viral particles were tittered using the AdEasy Viral Titer Kit (Agilent Technologies).

Statistical analysis

Data are presented as mean \pm S.D. The P-value was determined by two-tailed T-test. A P-value \leq 0.05 was considered statistically significant.

Supplementary Material

Refer to Web version on PubMed Central for supplementary material.

ACKNOWLEDGEMENTS

We thank A. Blais for Six1 antiserum, T. Sukonnik for in situ hybridization, J. Wythe for Cre/mT/mG embryos, J. Wylie for technical assistance, D. Miguel-Perez for animal husbandry, A. Holloway and A. Williams (Gladstone Bioinformatics core) for RNA-seq and microarray data analysis, L. Ta (Gladstone Genomics Core) for microarray experiments, C. Miller (Gladstone Histology Core) for histology, Bruneau lab members for helpful discussions, and Gary Howard for editorial assistance. This work was supported by a fellowship from the California Institute for Regenerative Medicine (P.D.-O.), a grant from the NIH (U01HL098179), the Lawrence J. and Florence A. DeGeorge Charitable Trust/American Heart Association Established Investigator Award (B.G.B.), and by William H. Younger, Jr. (B.G.B.). Animal work was supported by an NIH/NCRR grant (C06 RR018928) to the J. David Gladstone Institutes.

REFERENCES

1. Gluckman PD, Hanson MA, Buklijas T, Low FM, Beedle AS. Epigenetic mechanisms that underpin metabolic and cardiovascular diseases. *Nature reviews. Endocrinology*. 2009; 5:401–408.
2. Petronis A. Epigenetics as a unifying principle in the aetiology of complex traits and diseases. *Nature*. 2010; 465:721–727. [PubMed: 20535201]
3. Surface LE, Thornton SR, Boyer LA. Polycomb group proteins set the stage for early lineage commitment. *Cell stem cell*. 2010; 7:288–298. [PubMed: 20804966]
4. Margueron R, Reinberg D. Chromatin structure and the inheritance of epigenetic information. *Nat Rev Genet*. 2010; 11:285–296. [PubMed: 20300089]
5. Margueron R, Reinberg D. The Polycomb complex PRC2 and its mark in life. *Nature*. 2011; 469:343–349. [PubMed: 21248841]
6. Su IH, et al. Ezh2 controls B cell development through histone H3 methylation and Igh rearrangement. *Nat Immunol*. 2003; 4:124–131. [PubMed: 12496962]
7. Pereira JD, et al. Ezh2, the histone methyltransferase of PRC2, regulates the balance between self-renewal and differentiation in the cerebral cortex. *Proceedings of the National Academy of Sciences of the United States of America*. 2010; 107:15957–15962. [PubMed: 20798045]
8. Xu CR, et al. Chromatin "prepattern" and histone modifiers in a fate choice for liver and pancreas. *Science*. 2011; 332:963–966. [PubMed: 21596989]
9. Juan AH, et al. Polycomb EZH2 controls self-renewal and safeguards the transcriptional identity of skeletal muscle stem cells. *Genes & development*. 2011; 25:789–794. [PubMed: 21498568]
10. Guo C, et al. A Tbx1-Six1/Eya1-Fgf8 genetic pathway controls mammalian cardiovascular and craniofacial morphogenesis. *The Journal of clinical investigation*. 2011; 121:1585–1595. [PubMed: 21364285]
11. Heineke J, Molkenkin JD. Regulation of cardiac hypertrophy by intracellular signalling pathways. *Nature reviews. Molecular cell biology*. 2006; 7:589–600. [PubMed: 16936699]
12. Ahmad F, Seidman JG, Seidman CE. The genetic basis for cardiac remodeling. *Annual review of genomics and human genetics*. 2005; 6:185–216.
13. Bergmann O, et al. Evidence for cardiomyocyte renewal in humans. *Science*. 2009; 324:98–102. [PubMed: 19342590]
14. Margueron R, et al. Ezh1 and Ezh2 maintain repressive chromatin through different mechanisms. *Mol Cell*. 2008; 32:503–518. [PubMed: 19026781]
15. Shen X, et al. EZH1 mediates methylation on histone H3 lysine 27 and complements EZH2 in maintaining stem cell identity and executing pluripotency. *Mol Cell*. 2008; 32:491–502. [PubMed: 19026780]
16. Verzi MP, McCulley DJ, De Val S, Dodou E, Black BL. The right ventricle, outflow tract, and ventricular septum comprise a restricted expression domain within the secondary/anterior heart field. *Dev Biol*. 2005; 287:437–449.

17. Weiford BC, Subbarao VD, Mulhern KM. Noncompaction of the ventricular myocardium. *Circulation*. 2004; 109:2965–2971. [PubMed: 15210614]
18. Swynghedauw B. Phenotypic plasticity of adult myocardium: molecular mechanisms. *The Journal of experimental biology*. 2006; 209:2320–2327. [PubMed: 16731808]
19. Houweling AC, van Borren MM, Moorman AF, Christoffels VM. Expression and regulation of the atrial natriuretic factor encoding gene *Nppa* during development and disease. *Cardiovasc Res*. 2005; 67:583–593. [PubMed: 16002056]
20. McFadden DG, et al. A GATA-dependent right ventricular enhancer controls *dHAND* transcription in the developing heart. *Development*. 2000; 127:5331–5341. [PubMed: 11076755]
21. Takeuchi JK, et al. Chromatin remodeling complex dosage modulates transcription factor function in heart development. *Nat Commun*. 2011; 2:187. [PubMed: 21304516]
22. Kumar JP. The sine oculis homeobox (*SIX*) family of transcription factors as regulators of development and disease. *Cellular and molecular life sciences : CMLS*. 2009; 66:565–583. [PubMed: 18989625]
23. Li X, et al. Eya protein phosphatase activity regulates Six1-Dach-Eya transcriptional effects in mammalian organogenesis. *Nature*. 2003; 426:247–254. [PubMed: 14628042]
24. Schonberger J, et al. Mutation in the transcriptional coactivator *EYA4* causes dilated cardiomyopathy and sensorineural hearing loss. *Nat Genet*. 2005
25. Liu Y, Chu A, Chakroun I, Islam U, Blais A. Cooperation between myogenic regulatory factors and *SIX* family transcription factors is important for myoblast differentiation. *Nucleic acids research*. 2010; 38:6857–6871. [PubMed: 20601407]
26. Christodoulou DC, Gorham JM, Herman DS, Seidman JG. Construction of normalized RNA-seq libraries for next-generation sequencing using the crab duplex-specific nuclease. *Current protocols in molecular biology* / edited by Frederick M. Ausubel ... [et al.]. 2011 Chapter 4, Unit4 12.

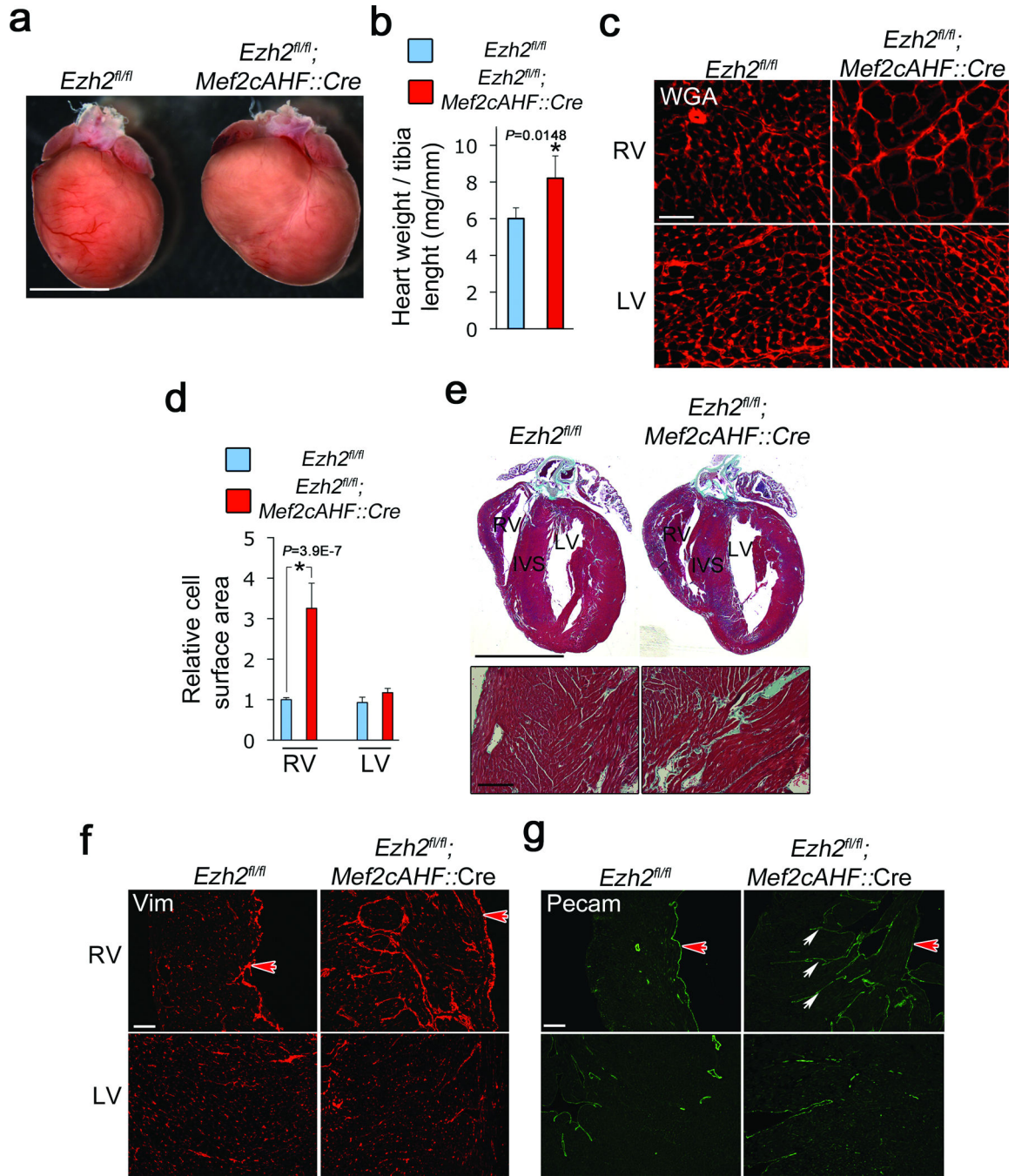


Figure 1. Ezh2 limits cardiac growth and fibrosis. (a) Adult mice in which Ezh2 was deleted in second heart field progenitors (*Ezh2^{fl/fl}; Mef2cAHF::Cre*) present hypertrophied right ventricle, with increased (b) heart weight to tibia length ratio (mg/mm), as compared to controls (*Ezh2^{fl/fl}*). *Ezh2^{fl/fl}* (blue bars) and *Ezh2^{fl/fl}; Mef2cAHF::Cre* (red bars). (c) Wheat germ agglutinin (WGA) staining of heart sections in control (*Ezh2^{fl/fl}*) or Ezh2-deficient (*Ezh2^{fl/fl}; Mef2cAHF::Cre*) right ventricle (RV) and left ventricle (LV). (d) Cardiomyocyte cell surface area in *Ezh2^{fl/fl}* (blue bars) or *Ezh2^{fl/fl}; Mef2cAHF::Cre* (red bars) hearts. (e) Tissue

disorganization and fibrosis, as revealed with Masson's trichrome staining. In **b** and **d**, bars represent the mean \pm S.D. of measurements from at least three hearts per genotype. * indicates $P < 0.05$. **(f)** Vimentin staining of RV and LV of *Ezh2^{fl/fl}* or *Ezh2^{fl/fl}; Mef2c^{AHF::Cre}* hearts. **(g)** Pecam staining showing invaginations of endocardium into myocardium (arrows). In **f,g**, the red arrow points to endocardial lining of the RV lumen. Reference bars in **(a)** and **(e)** (upper panel) = 0.5 cm; **(e)** (lower panel) = 100 μ m; **(c)** = 25 μ m; **(f)** and **(g)** = 100 μ m.

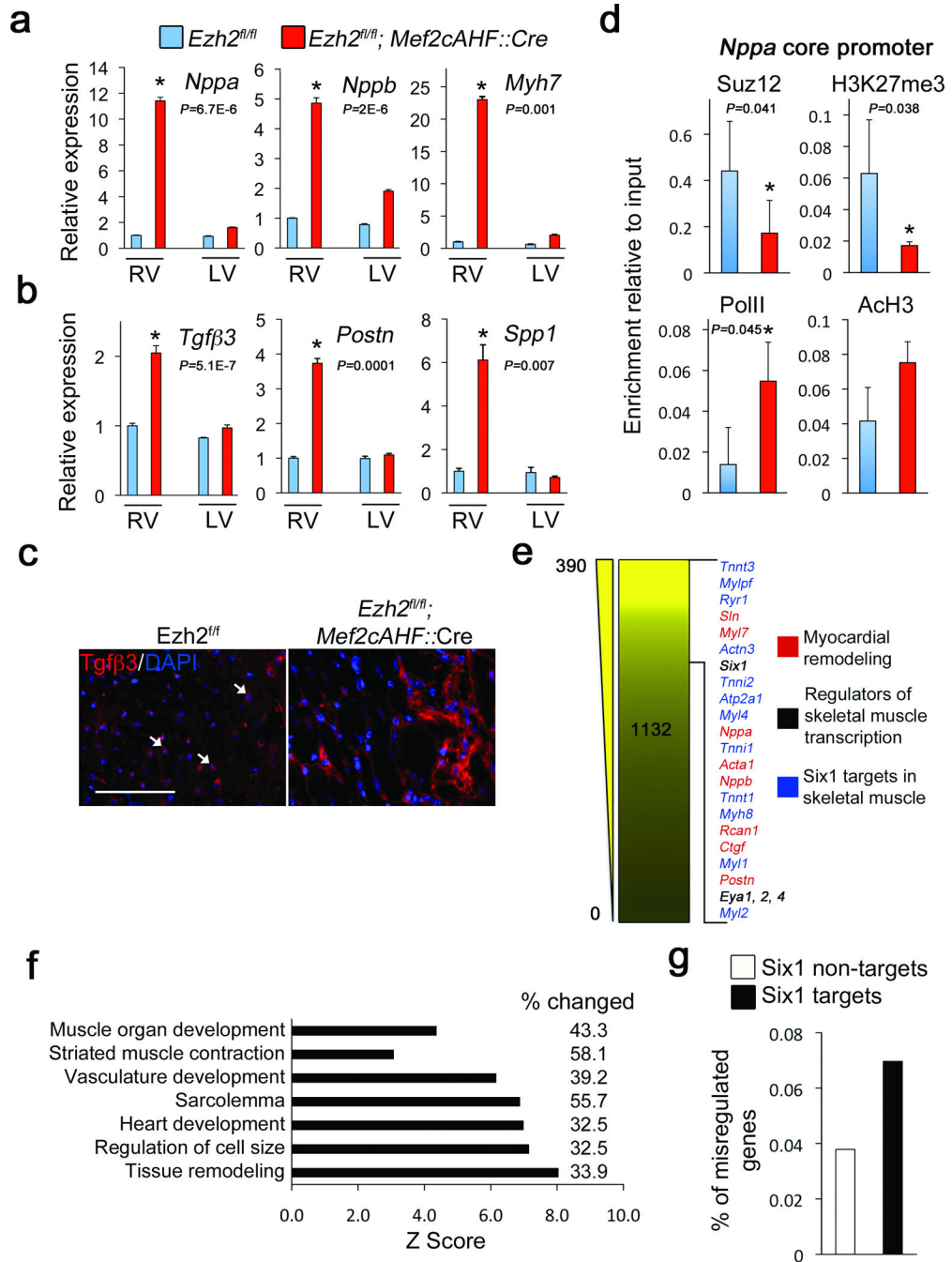


Figure 2. *Ezh2* represses expression of fetal genes, profibrosis factors and *Six1*. (a) QRT-PCR showing relative expression of *Nppa*, *Nppb* and *Myh7* mRNA. *Ezh2^{fl/fl}* (blue bars) and *Ezh2^{fl/fl}; Mef2cAHF::Cre* (red bars). (b) QRT-PCR showing expression of *Tgfβ3*, *Postn* and *Spp1*. (c) Immunofluorescence showing low levels of perinuclear *Tgfβ3* in control cardiomyocytes (arrows), and strong extracellular staining in the extracellular region in *Ezh2^{fl/fl}; Mef2cAHF::Cre* right ventricle (RV). Nuclei were counterstained with DAPI. (d) Chromatin immunoprecipitation for Suz12, H3K27me3, RNA PolIII, and acetylated histone H3 (ACh3)

on the *Nppa* core promoter in Ezh2-deficient Hearts (red bars), as compared with controls (blue bars). **e**, Heat map of 1132 upregulated genes identified by RNA-seq comparing Ezh2-deficient hearts to control hearts. Numbers at left indicate fold increase. Indicated genes were amongst the most upregulated. **f** Analysis of functional categories identified a high percentage of genes regulating skeletal muscle and tissue remodelling. **g** RNA-seq analyses showed a higher percentage of deregulated genes targeted by Six1, as compared to deregulated genes not targeted by Six1, in Ezh2-deficient hearts. Reference bars = 25 μ m. Bars in panels **(a)**, **(b)** and **(d)** represent the mean \pm S.D. from at least three biological replicates. * Indicates $P < 0.05$.

Author Manuscript

Author Manuscript

Author Manuscript

Author Manuscript

co-expressed *Six1* and *Actn3*. Arrows point to *Six1*-positive cardiomyocyte nuclei. LV: left ventricle. Reference bar = 25 μm . **(d)** Chromatin immunoprecipitation for Suz12, H3K27me3, RNA PolII, and acetylated histone H3 (AcH3) on the *Six1* core promoter in *Ezh2*-deficient Hearts (red bars), and controls (blue bars). Bars in panels **(a)** and **(d)** represent the mean \pm S.D. of at least three biological replicates. * Indicates $P < 0.05$.

Author Manuscript

Author Manuscript

Author Manuscript

Author Manuscript

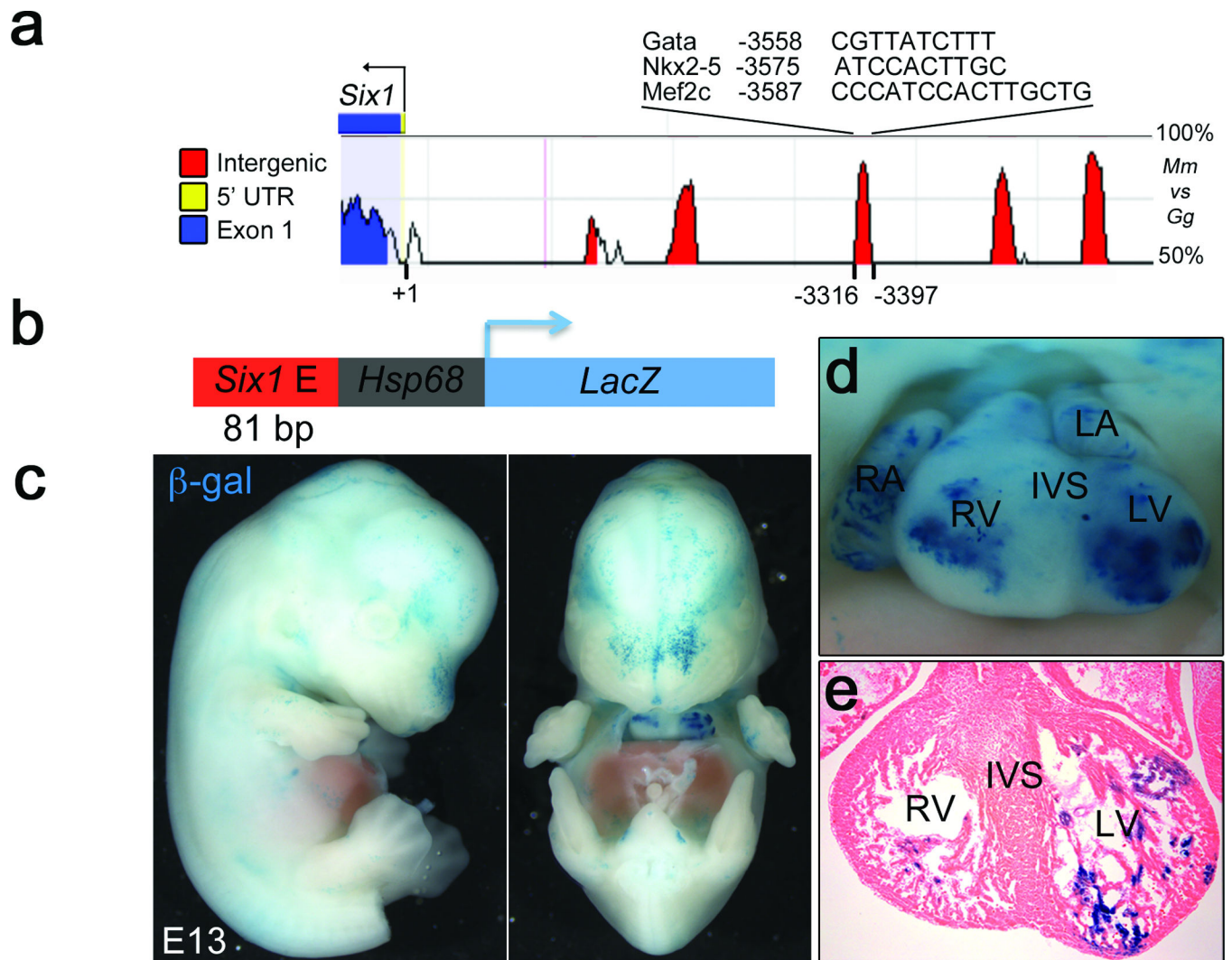


Figure 4. Six1 has differentiated myocardium expression potential. **(a)** rVista plot of the percentage of conservation between the mouse (*Mm*) and chicken (*Gg*) *Six1* upstream regulatory region. The indicated peak represents a highly conserved element including potential Nkx2-5, Mef2c and Gata binding motifs. **(b)** A LacZ reporter driven by the Hsp68 promoter and a 80bp DNA fragment including such a conserved element was injected into mouse blastocysts. **(c)** Lateral and frontal views of whole mount transgenic *Six1-hsp68-lacZ* embryos at E11.5 that were stained for β-galactosidase (β-gal) activity. **(d)** Close up of the heart from the same embryo. **(e)** Section from heart in g showing b-gal staining in ventricular myocardium. RA, LA, RV and LV: right and left atria, and ventricles, respectively.

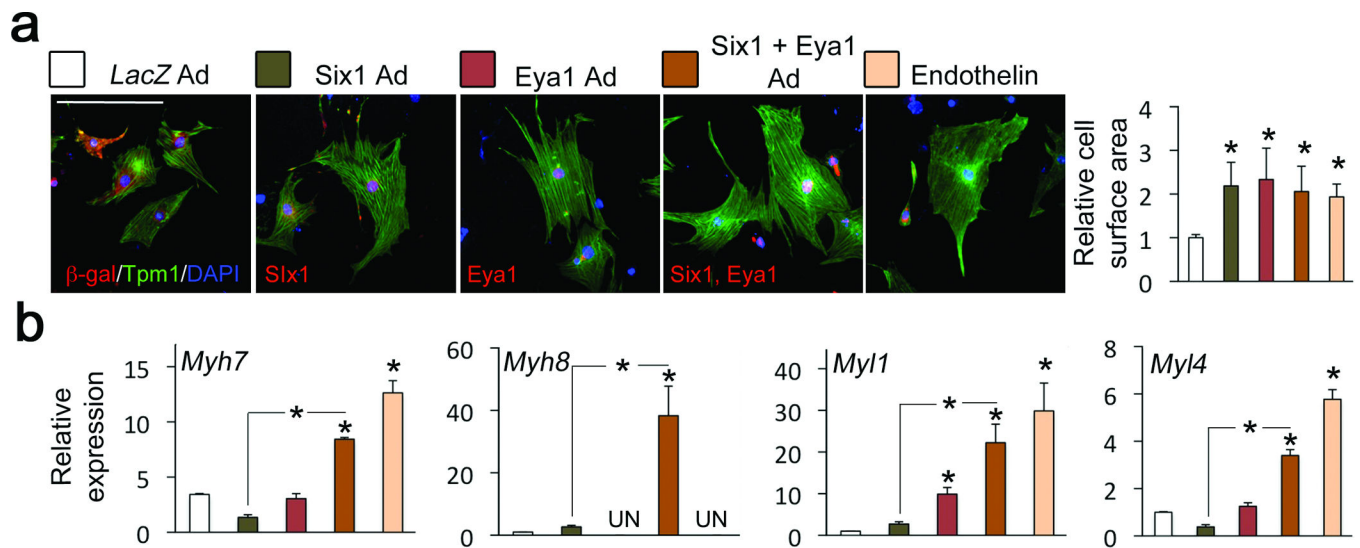


Figure 5.

Six1 induces cardiac hypertrophy and skeletal muscle gene expression in cardiomyocytes.

(a) Cardiac myocytes infected with adenoviruses (ad) expressing control cDNA (*lacZ*), *Six1*, or *Eya1*, or treated with Endothelin-1. Expression of *LacZ*, *Six1* and *Eya1*, was confirmed with staining for β -galactosidase (β -gal), and V5-tagged *Six1* and *Eya1*. Cardiomyocytes were stained for tropomyosin, and nuclei counterstained with DAPI. Graph shows average cell surface area. Bars represent the mean \pm S.D. from at least 100 myocytes measured. Reference bars = 10 μ m. (b) QRT-PCR of skeletal muscle genes on RNA from infected cardiomyocytes. Bars in (a,b) represent the mean \pm S.D. from at least three independent infections. * Indicates $P < 0.05$. LV: left ventricle

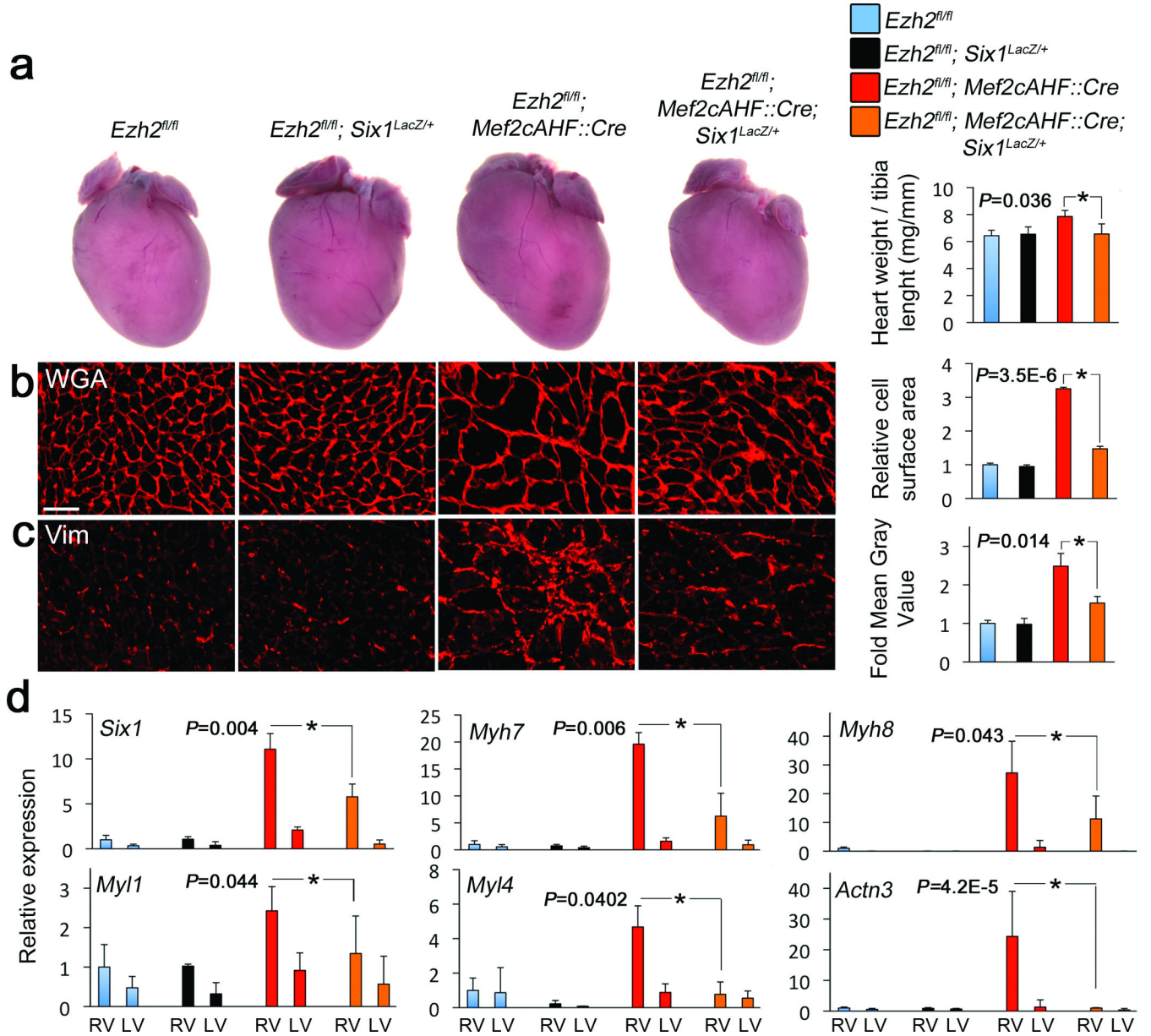


Figure 6. *Ezh2* limits cardiac hypertrophy and fibrosis by repressing *Six1*. (a) Whole heart images and heart mass, as represented by heart weight to tibia length ratio of *Ezh2* floxed (*Ezh2^{fl/fl}*), *Six1* heterozygous (*Ezh2^{fl/fl}; Six1^{LacZ/+}*), *Ezh2*-deficient mice (*Ezh2^{fl/fl}; Mef2c::Cre*), and *Ezh2*-deficient mice with decreased levels of *Six1* (*Ezh2^{fl/fl}; Mef2c::Cre; Six1^{LacZ/+}*) (b), Heart sections from mice with the same genotypes as in (a) stained with wheat germ agglutinin (WGA) and (c) vimentin. Graphs show the respective quantitations. (d) QRT-PCR for *Six1*, *Myh7*, *Myh8*, *Myl1*, *Myl4* and *Actn3*. Reference bars = 10 μ m. Bars represent the mean \pm S.D. from at least three hearts per genotype. * indicates $P < 0.05$.